Typhoon Haiyan. The nature and climatology of Haiyan was unique and Sidebar 4.2 is included to better document this event.

2) Atlantic Basin—G. D. Bell, C. W. Landsea, S. B. Goldenberg, R. J. Pasch, E. S. Blake, J. Schemm, and T. B. Kimberlain

(i) 2013 Seasonal activity

The 2013 Atlantic hurricane season produced 13 named storms, of which only 2 became hurricanes, and none became major hurricanes. The HURDAT2 1981–2010 seasonal averages are 11.8 tropical storms, 6.4 hurricanes, and 2.7 major hurricanes (Landsea and Franklin 2013). The 2013 season ties 1982 for the fewest hurricanes in the recent historical record from 1950 to present, and is the first season since 1994 with no major hurricanes. The entire life cycle of both hurricanes occurred within the period of 9–16 September.

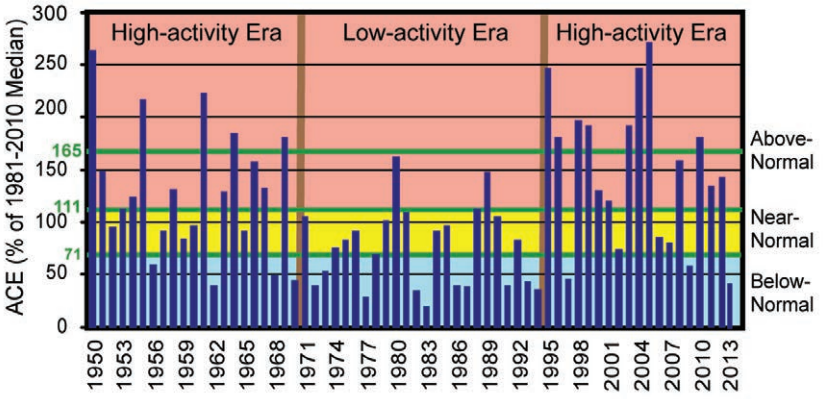

Fig. 4.8. NOAA's Accumulated Cyclone Energy (ACE) index expressed as percent of the 1981–2010 median value. ACE is calculated by summing the squares of the 6-hourly maximum sustained wind speed (kt) for all periods while the storm is at least tropical storm strength. Pink, yellow, and blue shadings correspond to NOAA's classifications for above-, near-, and below-normal seasons, respectively. The 165% threshold for a hyperactive season is indicated. Vertical brown lines separate high- and low-activity eras.

The seasonal accumulated cyclone energy (ACE) value (Bell et al. 2000) was only 39% of the 1981–2010 median (Fig. 4.8)[2]. This is the 10th lowest value since records began in 1950 and satisfies NOAA's criteria for a below-normal season (see http://www.cpc.ncep.noaa.gov/products/outlooks/background_information.shtml).

The 2013 ACE value, as well as the numbers of hurricanes and major hurricanes, are the lowest of the current high-activity era for Atlantic hurricanes that began in 1995 (Landsea et al. 1998; Goldenberg et al. 2001; Bell and Chelliah 2006; Bell et al. 2013). Thirteen seasons since 1995 (68%) have been above normal and only three (16%) have been below normal. Only one of these below-normal seasons (2013) occurred in the absence of El Niño, which is an indicator of how unusual the 2013 season was. In fact, the 2013 values for every parameter (except number of named storms) were below 1997, a year with one of the strongest El Niños in over 50 years. More details on the unusually quiet 2013 season can be found in Sidebar 4.1.

A main delineator between above- and below-normal seasons (Fig. 4.9) is the frequency of hurricanes and major hurricanes that originate as named storms within the main development region [MDR; green boxed region in Fig. 4.10a, which encompasses the tropical Atlantic Ocean and Caribbean Sea between 9.5° and 21.5°N (Goldenberg et al. 2001; Bell and Chelliah 2006)]. Only six named storms formed in the MDR during 2013, producing one hurricane (Humberto) and having a total ACE value that was 18% of the median. These numbers are comparable to the average MDR activity of a below-normal season,

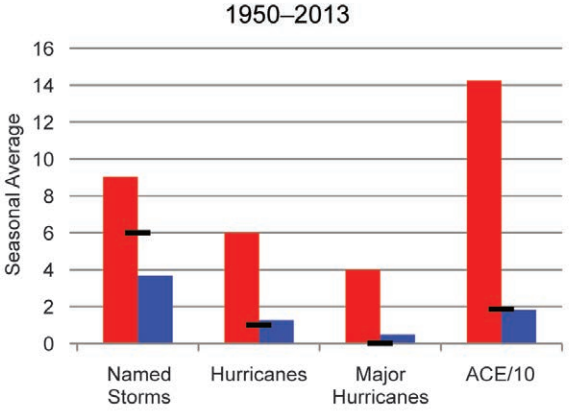

Fig. 4.9. Seasonal activity associated with storms first named in the Atlantic MDR. Red bars show the averages for above-normal seasons, blue bars show the averages for below-normal seasons, and black lines show the 2013 MDR activity. Season classifications are based on NOAA's criteria (see http://www.cpc.ncep.noaa.gov/products/outlooks/background_information.shtml).

[2] ACE is calculated by summing the squares of the six-hourly maximum sustained wind speed (knots) for all periods while the storm is at least tropical storm strength.

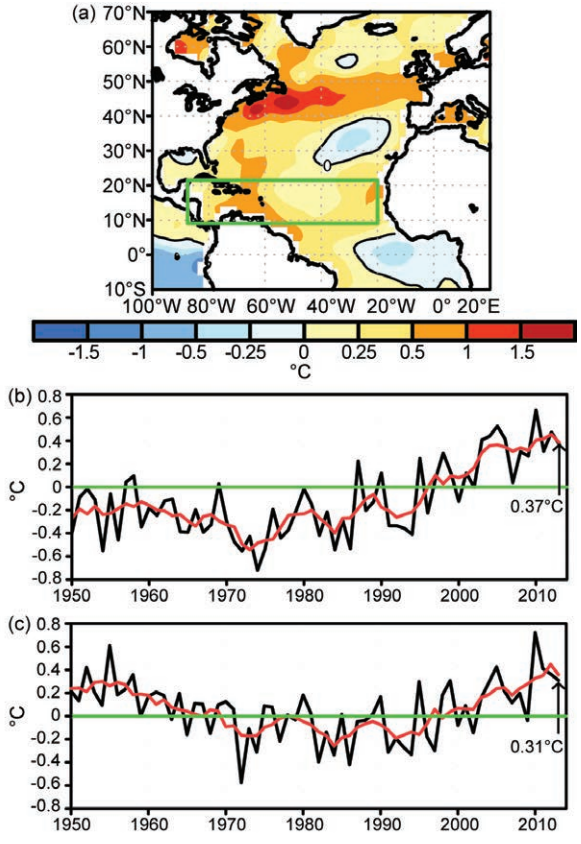

Fig. 4.10. (a) ASO 2013 SST anomalies (°C). (b) Time series during 1950–2013 of ASO area-averaged SST anomalies in the MDR [green box in (a)]. (c) Time series showing the difference between ASO area-averaged SST anomalies in the MDR and those for the entire global tropics (20°N–20°S). Red lines show a 5-pt. running mean of each time series. Anomalies are departures from the ERSST-v3b (Smith et al. 2008) 1981–2010 period monthly means.

and are at least six times lower than the above-normal season averages (six hurricanes and an ACE value of 142% of the median).

(ii) Storm tracks

The 2013 Atlantic hurricane season featured three distinct sets of storm tracks. The first was related to five named storms that formed over the central and eastern tropical and subtropical Atlantic. Only one of these storms made landfall—Tropical Storm Chantal in the Caribbean islands. The second set of tracks reflected three named storms that formed in the Bay of Campeche and made landfall in eastern Mexico. Of these storms, Ingrid was the only hurricane of the season to make landfall. The third set of tracks reflected two tropical storms that moved across the central Gulf of Mexico. One of these systems, Tropical Storm Andrea, was the first named storm of the season and the only U.S. landfalling storm, striking northwestern Florida before moving across southeastern Georgia and South Carolina and becoming extratropical in North Carolina.

(iii) Atlantic sea surface temperatures

SSTs in the MDR were above average during the peak months (August–October, ASO) of the season, with the largest departures (between +0.5° and +1.0°C) observed across the eastern half of the Caribbean Sea (Fig. 4.10a). The mean SST departure within the MDR was +0.37°C. This value is the seventh highest in the 1950–2013 record (Fig. 4.10b) and is 0.3°C warmer than the average departure for the entire global tropics (Fig. 4.10c). This relative warmth within the MDR has been present since 1995 and is a feature of the warm phase of the Atlantic multidecadal oscillation (AMO; Enfield and Mestas-Nuñez 1999; Goldenberg et al. 2001; G. D. Bell et al. 2011, 2013), and this makes the relative inactivity for the season all the more unusual.

(iv) Atmospheric circulation

The below-normal Atlantic hurricane season was largely the result of a set of exceptionally nonconducive atmospheric conditions within the MDR. One suppressing factor was the presence of strong (≥8 m s^{-1}) 200–850 hPa vertical wind shear across most of the tropical Atlantic Ocean, Caribbean Sea, and Gulf of Mexico (Fig. 4.11), with above-average shear observed across the Caribbean Sea and Gulf of Mexico (not shown). Areas of weaker shear were confined to the southeastern MDR and Bay of Campeche. This signal is in stark contrast to a typical above-normal season, which features weak shear across large portions of the MDR.

Also during ASO 2013, large areas within the MDR experienced anomalous upper-level conver-

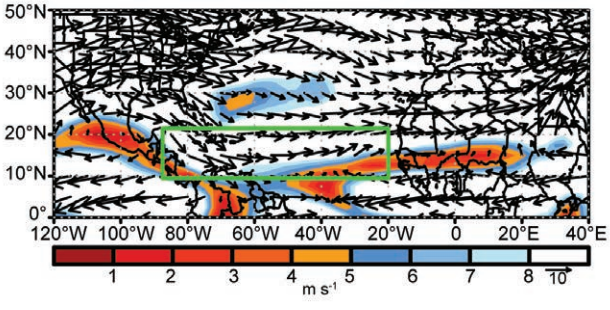

Fig. 4.11. ASO 2013 vertical wind shear magnitude and vectors (m s^{-1}). Shading indicates areas where the vertical wind shear magnitude is ≤ 8 m s^{-1}. Green box denotes the MDR. Vector scale is below right of color bar.

gence and lower-level divergence (Fig. 4.12a), along with anomalous mid- and low-level sinking motion (Fig. 4.12b) and drier air (Fig. 4.12c). None of these conditions are conducive to TC formation. Furthermore, the conducive phase of the MJO (Mo 2000) did not substantially offset these non-conducive conditions since it was present for only a brief period in early September and mid-October (see Fig. 4.6).

Climate factors such as El Niño and the cold phase of the AMO can produce non-conducive conditions within the MDR, but neither of these factors were present during ASO 2013. Instead, the observed conditions were related to a strong and persistent anomalous 200-hPa wave pattern that extended from North America to the eastern North Atlantic (Fig. 4.13a). This wave pattern had no apparent large-scale climate links. Key features of this pattern (ridge and trough axes shown by thick black lines in Fig. 4.13c) include: (1) an amplified ridge extending northward from Mexico; (2) a downstream amplified trough over the western subtropical North Atlantic and Caribbean Sea (called the tropical upper-tropospheric trough, TUTT); and (3) an amplified ridge over the central and eastern subtropical North Atlantic.

This wave pattern contributed to the non-conducive conditions within the MDR in two primary ways. First, its associated northwesterly flow from the Great Lakes to the southern Caribbean Sea (Fig. 4.13a) produced anomalous northerly and northwesterly vertical wind shear across the entire Caribbean Sea, resulting in the anomalously strong shear observed across the western half of the MDR (Fig. 4.13b).

Second, the strong curvature of the wave pattern was likely the primary contributor to the anomalous upper-level convergence and sinking motion across

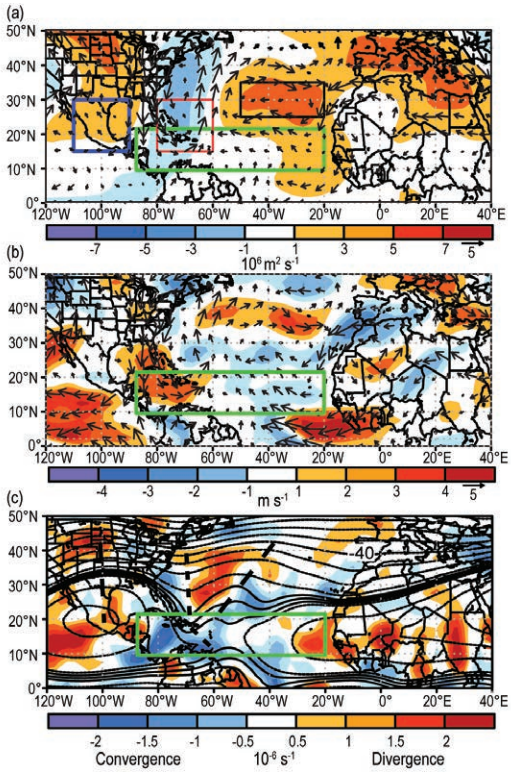

Fig. 4.13. ASO 2013 circulation and anomalies: (a) 200-hPa anomalous streamfunction (shaded, ×10^{-6} m^2 s^{-1}) and wind vector (m s^{-1}), (b) 200–850 hPa anomalous magnitude of vertical wind shear and anomalous shear vector (m s^{-1}), and (c) total 200-hPa streamfunction (contours, interval is 5 × 10^6 m^2 s^{-1}, with additional solid contours at an interval of 1 × 10^6 m^2 s^{-1}) and anomalous divergence (shaded, ×10^{-6} s^{-1}). Boxes in (a) show index regions for Figs. 4.14 and 4.15. Vector scales for (a, b) are shown below right of color bar. Thick dashed lines in (c) identify ridge and trough axes of persistent wave pattern discussed in text. Green boxes in all panels indicate the MDR. Anomalies are based on the 1981–2010 climatology.

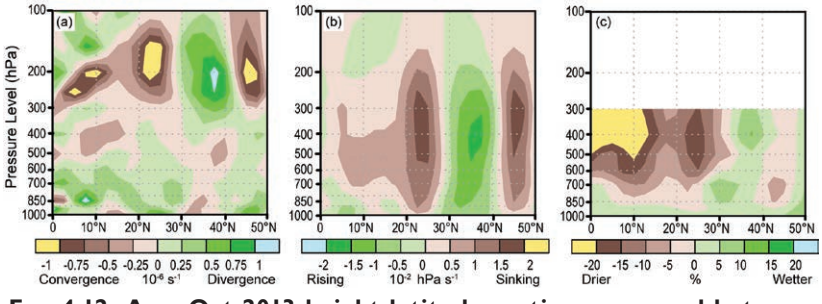

Fig. 4.12. Aug–Oct 2013 height-latitude sections averaged between 40°–60°W of (a) anomalous divergence (×10^{-6} s^{-1}), (b) anomalous vertical velocity (×10^{-2} hPa s^{-1}), and (c) percent of normal specific humidity. Green shading indicates anomalous divergence, anomalous rising motion, and increased moisture, respectively. Brown shading indicates anomalous convergence, anomalous sinking motion, and decreased moisture. Climatology and anomalies are with respect to the 1981–2010 period monthly means.

the western and central MDR. This area was part of a much larger region of upper-level convergence located between the amplified ridge (over Mexico) and the downstream TUTT axis, which is an area within midlatitude wave patterns known for upper-level convergence and descending motion. Similarly, a strong ridge within the eastern portion of the wave pattern contributed to the anomalous upper-level convergence and sinking motion over the central MDR, and also over the central subtropical North Atlantic north of the MDR.

Given these relationships, it is of interest to quantify the relative strength of the 200-hPa wave pattern during ASO 2013, along with its historical frequency of occurrence. The analysis is based upon ASO standardized streamfunction indices for the three regions shown in Fig. 4.13a [Mexico (blue box), the Caribbean Sea and western subtropical North Atlantic (orange box), and the eastern North Atlantic (black box)].

The index time series (dating back to 1970) shows that streamfunction anomalies within the Caribbean Sea region (Fig. 4.14, orange bars) typically have the same sign as those in both the Mexico (Fig. 4.14a, blue bars) and east Atlantic (Fig. 4.14b, black bar) regions. These relationships are reflected in their strong index correlations (0.86 and 0.73, respectively). In contrast, the ASO 2013 anomalies in the Caribbean Sea region had an opposite sign of the other two regions. There is only one other instance in the record (the below-normal 1994 season which featured three hurricanes, no major hurricanes, and an ACE of 35% of the median) in which a similar wave pattern existed with the amplitudes of all three indices exceeding 0.25 standard deviations.

An examination of the differences in index amplitudes between the three regions shows that the ASO 2013 wave pattern was of record strength (Figs. 4.15a,b). Similarly, the standardized index that is the sum of the anomaly differences from Figs. 4.15a and b (Fig. 4.15c) was also of record strength (+3 standard deviations), exceeding the next largest value (+2 standard deviations during ASO 1994) by a full standard deviation.

The analysis shows that the exceptionally non-conducive conditions within the MDR during ASO 2013 were linked to a rare (only twice since 1970) upper-level wave pattern of record strength that extended from Mexico to the eastern North Atlantic. It is of note that El Niño was present when this pattern last occurred in ASO 1994, but this was not the case during 2013.

This wave pattern does not have a known relationship to other climate factors and it therefore has a low probability of prediction on seasonal time scales.

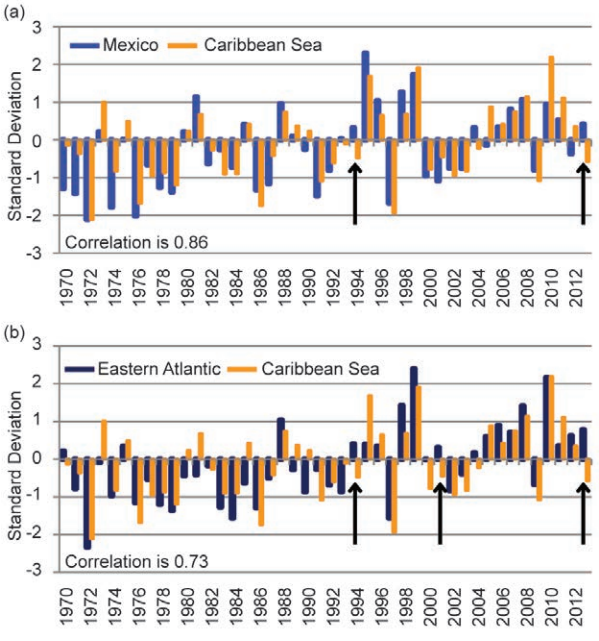

Fig. 4.14. ASO standardized streamfunction indices for the period 1970–2013 averaged over the boxed regions shown in Fig. 4.13a. Panel (a) shows indices for the Mexico (blue) and Caribbean Sea (orange) regions and panel (b) shows indices for the eastern Atlantic (black) and Caribbean Sea (orange) regions. The indices are calculated by first standardizing the ASO streamfunction anomalies at each grid point, and then standardizing the area-averaged value of the standardized grid-point anomalies. The correlations between the Mexico and Caribbean Sea indices and between the Eastern Atlantic and Caribbean Sea indices are given in panels (a) and (b), respectively. All standardizations are based on the 1981–2010 climatology.

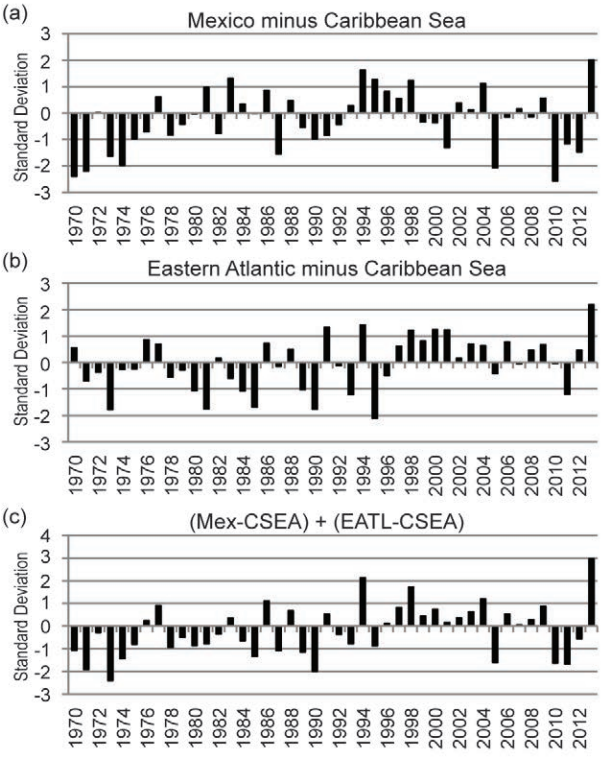

Fig. 4.15. ASO standardized indices for the period 1970–2013 based on (a) the Mexico minus Caribbean Sea indices from Fig. 4.14a, panel (b) the east Atlantic minus the Caribbean Sea indices from Fig. 4.14b, and (c) the indices in panel (a) minus those in (b). All standardizations are based on the 1981–2010 climatology.

Based on this analysis and on the ongoing warm phase of the AMO, the suppressed 2013 Atlantic hurricane season provides no indication that the current high-activity era for Atlantic hurricanes has ended.

3) Eastern North Pacific and Central North Pacific Basins—M. C. Kruk, C. J. Schreck, and T. Evans

(i) Seasonal activity

The Eastern North Pacific (ENP) Basin is officially split into two separate regions for the issuance of warnings and advisories by NOAA's National Weather Service. NOAA's National Hurricane Center is responsible for issuing warnings in the eastern part of the basin that extends from the Pacific Coast of North America to 140°W, while NOAA's Central Pacific Hurricane Center in Honolulu, Hawaii, is responsible for issuing warnings in the central North Pacific (CNP) region between 140°W and the dateline. This section summarizes the TC activity in both warning areas using combined statistics, along with information specifically addressing the observed activity and impacts in the CNP region.

The ENP/CNP hurricane season officially spans from 15 May to 30 November. Hurricane and tropical storm activity in the eastern area of the basin typically peaks in September, while in the central Pacific TC activity normally reaches its seasonal peak in August (Blake et al. 2009). During the 2013 season, a total of 20 named storms formed in the combined ENP/CNP Basin, with only 2 of these forming in the CNP (very close to the dateline). This total included nine hurricanes and one major hurricane. The 1981–2010 IBTrACS seasonal averages for the basin are 16.5 named storms, 8.5 hurricanes, and 4.0 major hurricanes.

An above-normal number of five named storms developed or entered into the CNP during 2013 (Fig. 4.16). Although half the TCs that formed in 2013 reached hurricane intensity, the ACE index for 2013 indicates many of the storms were weak and short-lived, with a seasonal value of only 70.1 × 10^4 kt^2 (Fig. 4.16), which is well below the 1981–2010 mean of 137.0 × 10^4 kt^2 (Bell et al. 2000; Bell and Chelliah 2006).

(ii) Environmental influences on the 2013 season

Figure 4.17 illustrates the background conditions for TC activity in the ENP and CNP during 2013. Consistent with the marginal La Niña conditions, weak cool SST anomalies were observed near the equator and along the Central American coast (Fig. 4.17a). Most of the TCs formed over an area of warm SST anomalies to the north off the Mexican coast. This also coincided with a broad region of enhanced

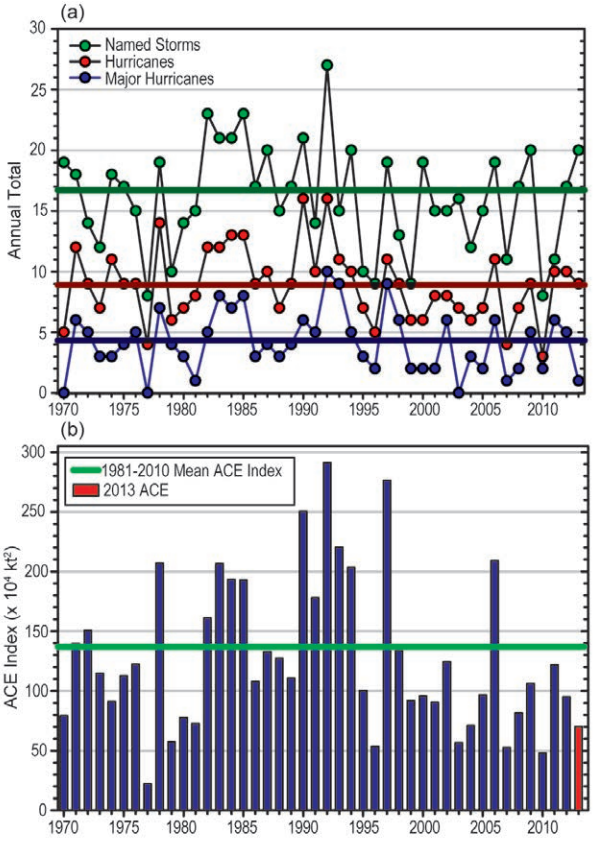

Fig. 4.16. Seasonal TC statistics for the ENP basin over the period 1970–2013: (top) number of named storms, hurricanes, and major hurricanes, and (bottom) the ACE Index (×10^4 kt^2)with the seasonal total of 2013 highlighted in red. The time series shown includes the corresponding 1981–2010 base period means for each parameter.

convection that extended from 140°W eastward to the Gulf of Mexico (Fig. 4.17b). Meanwhile, the ITCZ was generally suppressed and shifted northward, as indicated by the positive outgoing longwave radiation (OLR) anomalies along 5°N and negative anomalies near 12°N. Vertical wind shear magnitudes were generally close to their climatological values (Fig. 4.17c); however, the vertical wind shear anomalies were generally easterly in the ENP, which might have also favored cyclogenesis.

Figure 4.17d shows a broad area of 850-hPa westerly anomalies near the equator, with easterly anomalies to the north, similar to what occurred in 2012 (Diamond 2013). This combination produced the region of enhanced cyclonic vorticity within which most of the ENP storms developed. Many of these storms developed where the enhanced vorticity intersected the westerly anomalies. The westerlies could have strengthened easterly wave activity in this region through barotropic energy conversion